

# Influence of Heat Treatment of 30MnB5 Steel on its Micromechanical Properties and Resistance to Abrasion Wear

Myroslav Khoma<sup>a</sup>, Vasyl Vynar<sup>a</sup>, Chrystyna Vasyliv<sup>a,\*</sup>, Vadym Zakiev<sup>b</sup>, Bohdan Datsko<sup>a</sup>, Myron Golovchuk<sup>a</sup>

<sup>a</sup>Karpenko Physico-Mechanical Institute, 79060, Lviv, 5, Naukova str., Ukraine,

<sup>b</sup>National Aviation University, 03058, Kyiv, 1, Liubomyra Huzara ave. Ukraine.

## Keywords:

Boron-containing steel  
Heat treatment  
Dynamic indentation  
Scratch test  
Abrasive wear  
Microstructure

\* Corresponding author:

Chrystyna Vasyliv   
E-mail: [chrystyna.vasyliv@gmail.com](mailto:chrystyna.vasyliv@gmail.com)

Received: 23 June 2021

Revised: 30 July 2021

Accepted: 15 February 2022

## ABSTRACT

The microstructure evolution of the 30MnB5 steel, tempered at the different temperatures, the micromechanical properties and wear resistance was studied.

The correlation between results of sclerometry and wear resistance of steel was found. Minimal work of plastic deformation ( $29.42 \cdot 10^{-8}$  J) accompanies the maximal wear resistance of steel. This makes it possible to use sclerometry as an express method for testing steel for wear resistance after various types of heat treatment.

The abrasive wear resistance of 30MnB5 steel depends on its hardness which provides resistance of material to micro-cutting by abrasive grain. Maximal wear resistance of steel is observed after quenching and tempering at 200°C, when its hardness is 54 and 49 HRC.

The abrasive wear of quenched and tempered at 200°C steel 30MnB5 is the result of micro-cutting and micro-ploughing. The plastic deformation, displacement of material along the grooves, pit holes and chipping of the brittle components are observed on the friction surface of steel after tempering at 400°C and 600°C. Surface damage at the friction tests with an unfixed abrasive is less than with a fixed abrasive.

© 2022 Published by Faculty of Engineering

## 1. INTRODUCTION

The durability of highly loaded machine elements in agriculture, transport, mining, metalworking industry depends on wear resistance of structural materials [1-3]. Abrasive wear constitutes about 50% of the total wear of machine elements, working in these fields [2]. It is recommended to

use high-strength steels with a martensite structure and a yield strength >1200 MPa to ensure high performance properties of cutting parts [4]. High-strength steels are obtained by economically alloying of medium-carbon steels with manganese (1.1...1.5%), chromium (0.1... 0.6%), boron (0.0003... 0.01 %), microalloying with Mo, Ti, Nb, V and corresponding heat treatment [5-7]. Alloying

with boron (along with vanadium, titanium, niobium, rare earth metals, etc.) opens wide opportunities to produce economically alloyed steels, which characteristics exceed the properties of traditional alloyed steels [8-11]. Unlike other elements, addition of  $10^{-4}$ - $10^{-3}\%$  of boron significantly improves the quality of the metal. The effect of boron at this concentration on the hardenability and toughness of low- and medium-carbon alloy steels corresponds to the effect of alloying by 100-300 times more content of chromium, manganese, molybdenum, or nickel. This effect is created by "chemically soluble" boron, dissolved in the matrix and connected in iron carboborides  $Fe_{23}(B,C)_6$  and  $Fe_3(B,C)$  [10,11]. When a boron concentration in low- and medium-carbon steels is  $<0.005\%$ , carbides are sufficiently dispersed, maintain coherence with the matrix and inhibit the formation of ferrite at the grain boundary.

Heat treatment is a significant process for steels to obtain the optimal microstructure, which has a significant influence on the mechanical properties, especially on the hardness, and wear resistance [4,12]. The martensitic structure provides the necessary strength of steel, but detailed choice of modes of quenching and subsequent tempering helps to maintain an acceptable level of ductility and toughness ( $\delta = 5-15\%$ ). A controlled proportion of residual austenite is introduced into the high-strength martensitic structure after tempering. Even 10% of residual austenite improves ductility of strength steel and increases its wear resistance due to the heterogeneity of the two-phase structure. The tempering is the complex process, which includes the formation of  $\epsilon$ -carbides  $Fe_xC$ , the decomposition of residual austenite, the formation of cementite. The development of low-temperature tempering modes is quite a difficult task and depends on the composition of the steel.

The effect of different tempering temperature on the abrasive wear properties of boron steels is presented in [1-4,12]. It was found, that direct quenched steels showed slightly lower mass loss at abrasive wear, than tempered steels. Wear performance was mainly controlled by the initial hardness of steel and the combination of high hardness and toughness [12]. A correlation between the grain size, structure of low-alloy boron steels and the intensity of wear processes was found [1]. With an increase in austenite grain size, the intensity of wear increases. Wear of steel is the result of micro-cutting, micro-chips removal and micro plowing.

Some studies have been carried out regarding the high temperature abrasive wear behavior of boron steel [2,13]. The wear results were correlated to the hot hardness of material. Boron steel shows a reduced wear rate from  $20^\circ C$  to  $400^\circ C$  attributed to an increased toughness and formation of wear-protective tribolayers. The worn surface was plastically deformed during the wear process, resulting in a strain hardened layer.

The mechanical properties of steel in the micro/nanovolumes of surface and peculiarities of abrasive damage can be evaluated by the nanoindentation method and nanoscratch. This technique is used to measure on thin films or small volumes of materials mechanical parameters such as Young's modulus, hardness, residual stresses etc. [14-16]. Methods make it possible to assess the depth of damage of the material by abrasive, the characteristics of the destruction, the parameters of elasticity and plasticity. Electron microscopy in combination with nanoindentation provides the information about local mechanical properties of materials.

Boron-alloyed steel 30MnB5 is used for the manufacture of cutting parts for agricultural machinery [17-18]. Boron in low concentrations up to  $0.005\%$  is dissolved in the matrix of steel and forms compounds of type  $Me_{23}(B,C)_6$  and  $Fe(B,C)$ . Boron significantly increase the hardenability of steel. If boron compounds are sufficiently dispersed to maintain coherence with the matrix, they inhibit the formation of ferrite at the boundaries of austenitic grains. Minor impurities of boron cause significant dispersion of grains, increase hardness and wear resistance of steel due to strengthening of grains by borides [19].

Changes of the microstructure and micromechanical parameters of steel after heat treatment determine its exploitation characteristics, especially tribological behavior. This issue requires more detailed research.

The purpose of this paper is to determine the microstructure evolution of the 30MnB5 steel, tempered at different temperatures, its micromechanical properties and wear resistance under the conditions of dry abrasive friction with fixed and unfixed abrasive.

## 2. MATERIALS AND RESEARCH METHODS

### 2.1 Materials

Steel 30MnB5 in the state of delivery and after heat treatment (own research) was investigated. The chemical composition of steel 30MnB5 (according to Standard EN10083-3) is presented in the Table 1.

**Table 1.** The chemical composition of the test steel 30MnB5, wt.% (Standard EN10083-3).

C	Si	Mn	P	S	B	Fe
0.27-0.33	≤0,4	1.15-1.45	≤0.025	≤0.015	0.0008-0.0050	Bal.

Heat treatment was performed in a muffle furnace. Quenching scheme: heating to a temperature of 900°C for 60 min, holding for 10 min, cooling in water; tempering scheme: heating to a temperature of 200, 400 and 600°C - for 120, 120, 20 and 10 min, respectively, exposure for 10 minutes, cooling with an oven.

Rockwell hardness tester TKP-1 was used to measure hardness.

### 2.2 Micromechanical characterization

Micromechanical tests were performed on a Nano Indenter II nano-hardness tester from MTS Systems Corporation (USA) with a Berkovich indenter at a load of 5 mN. The rate of the load was constant and equal to 0.2 mN/s [16]. The method is based on the automatic registration of the load diagram  $P = f(h)$ , where  $P$  is the load on the indenter,  $h$  is the depth of its penetration into the surface of the investigated material (Fig. 1). Hardness is determined at the time of maximum penetration of the indenter ( $h_{max}$ ), i.e. before the elastic recovery of the material. It is an advantage of the method. The diagram gives information about the work of the indenter to overcome the resistance of the material  $A_{plast}$  (area under the load branch) and the work to restore its properties  $A_{elast}$  (area under the unloading branch) (Fig. 1).

The value of microhardness by Mayer is found as a ratio of the maximum load  $P_{max}$  to the area of the projection print  $A$ .

Therefore, the next micromechanical parameters were determined:  $H$  - microhardness after Mayer;

$A_{plast}$  - work of the indenter to overcome the resistance of the material (area under the load branch of diagram);  $A_{elast}$  - the work of elastic deformation (area under the unloading branch).

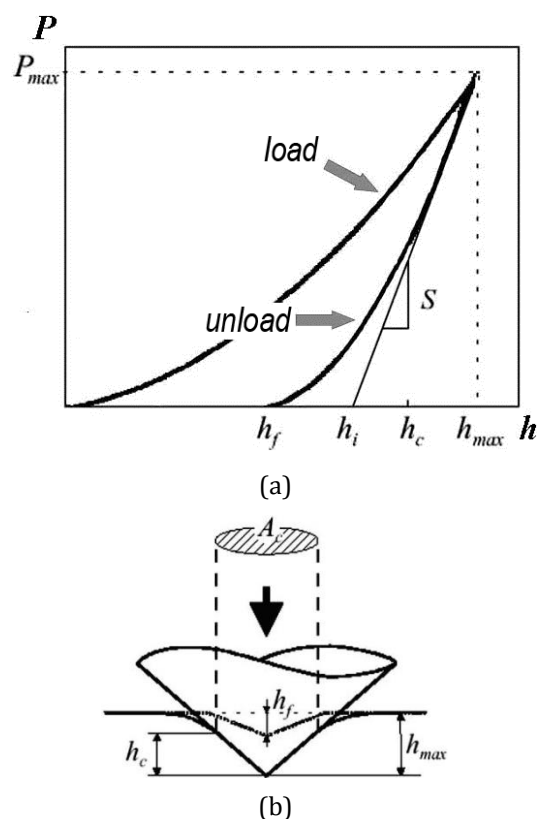


**Fig. 1.** The loading diagram (a) and an imprint cross section (b) at dynamic indentation [16]:  $h_{max}$ ,  $h_c$ ,  $h_f$  – the maximum penetration of a tip, elastic and plastic components of deformation,  $S$  is the tangent of the inclination angle of the unloading curve initial part.

### 2.3 Wear test

The wear resistance of steel with using of friction method with fixed and unfixed abrasive was investigated. In the first case, an abrasive disk with a diameter of 150 mm and a width of 8 mm was used as a counterbody. It was made from electrocorundum of medium soft hardness CM-2 on a ceramic base 7K15 (Fig. 2a).

The scheme of apparatus for the friction test with unfixed abrasive [19] is shown in Fig. 2b. The size of the sample is 30×30×50 mm, the diameter of the rubber disk is 48 mm, the width is 15 ± 0.1 mm. Test mode: load  $P = 2.40$  N, rotation speed 160 rpm, abrasive – sand with a grain size of 200-1000 μm, test time – 15 min. Before testing, the abrasive was fractionated and dried. 3 samples per point were used for the tests.

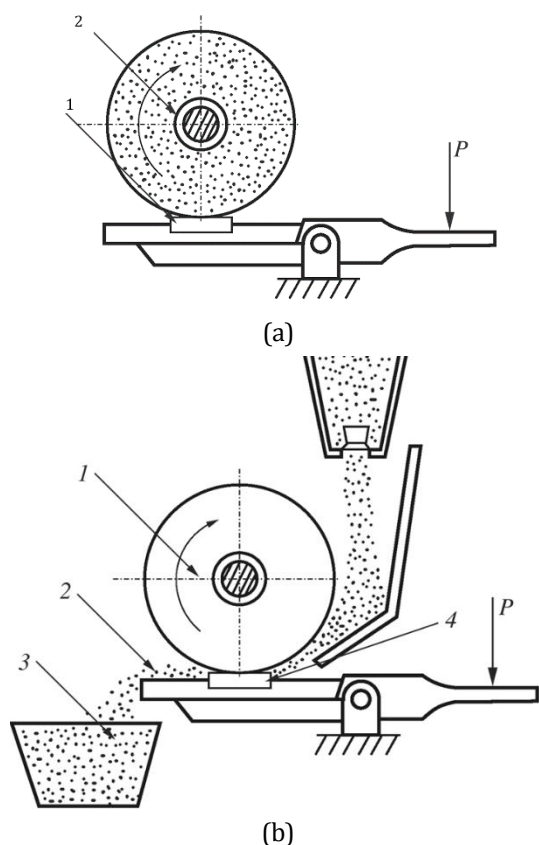


**Fig. 2.** Schematic of the apparatus for the friction test with fixed (a) and unfixed abrasive (b) [20]: 1 - sample; 2 - abrasive wheel, 2' - rubber disk; 3 - sand; 4 - capacity for cleaning abrasive, P - applied load.

The scratch method was used to assess the resistance of material to abrasive wear. It is based on continuous recording of the friction force at the movement of the indenter over the surface under a load 1 N and speed 0.2 mm/s. The method was combined with the determination of the friction force, volume of the material, displaced by the indenter and parameters of the surface roughness, which was formed at the scratch bottom [16]. Non-contact interference 3D profilograph “Micron-alpha” was used to obtain the parameters of the surface roughness and scratch profile.

Metallographic analysis was performed using a scanning electron microscope EVO-40XVP (Carl Zeiss) with a system of microanalysis on energy-dispersive X-ray spectrometer INCA ENERGY 350. The weight losses of 30MnB5 steel at the friction tests was determined gravimetrically.

The surface of the samples after milling was processed with grinding skin to roughness  $R_z = 2,5 \mu\text{m}$  for nanoindentation and friction. Standard preparing of the samples for electron microscopy measurements was used.

### 3. RESULTS AND DISCUSSION

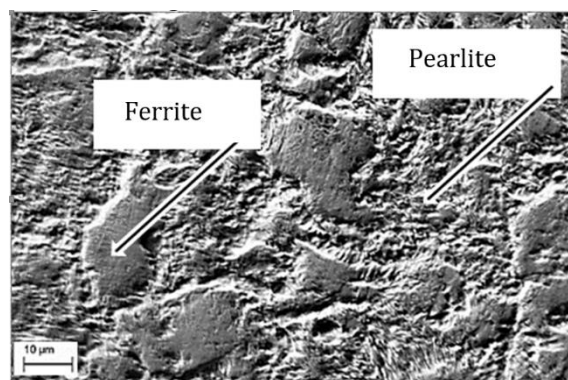
#### 3.1 Microstructure and mechanical properties

SEM images of the steel 30MnB5 after different thermal treatment are shown in Fig. 3. The structure of steel in the delivery state – the composition of ferrite and pearlite (Fig. 3a), the grain size is  $\sim 5\text{-}20 \mu\text{m}$  and its Rockwell hardness is  $\sim 22$  HRC (Table 2). After quenching from a temperature of  $900^\circ\text{C}$  the microstructure of the steel mainly consists of martensite, hardness increases to  $\sim 54$  HRC.

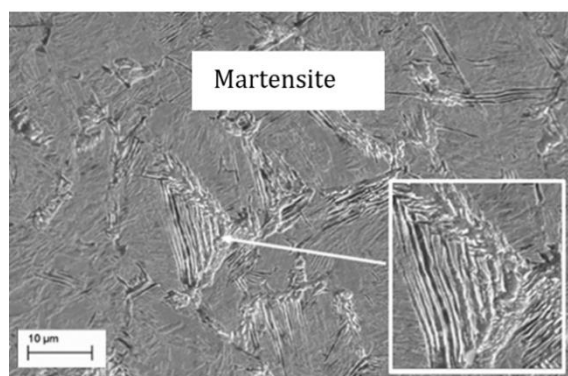
**Table 2.** Hardness of steel 30MnB5 after different heat treatment.

Heat treatment	HRC
Delivery state	22
Quenching in water from $900^\circ\text{C}$	54
Quenching and tempering at $200^\circ\text{C}$	49
Quenching and tempering at $400^\circ\text{C}$	32
Quenching and tempering at $600^\circ\text{C}$	28

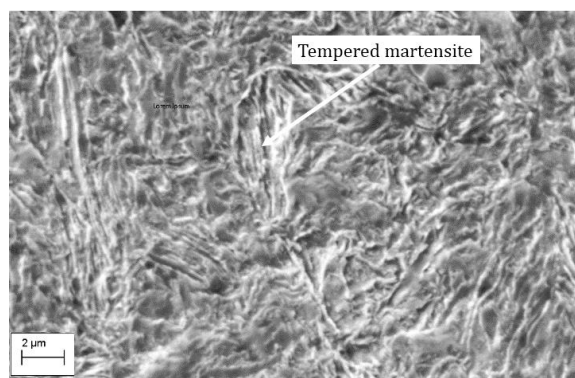
Martensite needles of different sizes were found in the structure, which are etched in different ways (Fig. 3b). The image at the bottom right corner in Fig. 3b is the amplification of the region where the larger needles (up to  $15 \mu\text{m}$  long) are etched. These needles are probably formed at the beginning of the martensitic transformation.



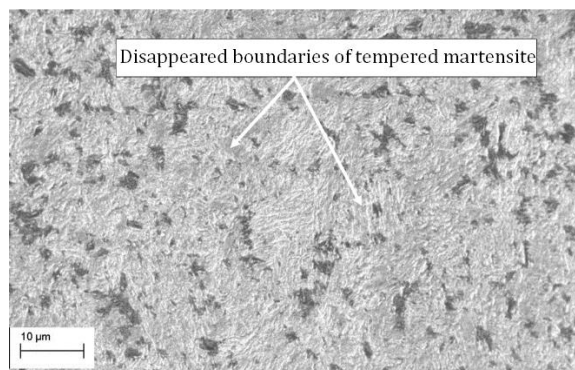
(a)



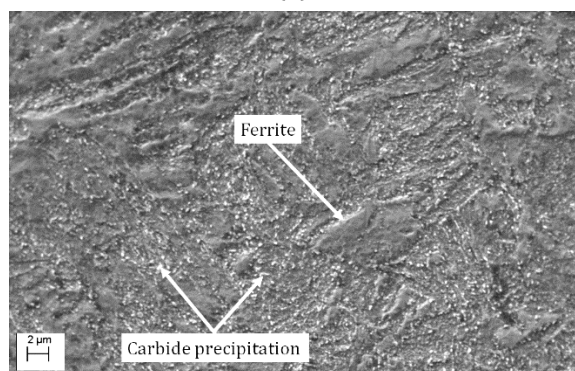
(b)



(c)



(d)



(e)

**Fig. 3.** The microstructure of steel 30MnB5: (a) - delivery state; (b) - quenching in water from a temperature of 900°C; (c) - quenching and tempering at 200°C, (d) - quenching and tempering at 400°C, (e) - quenching and tempering at 600°C.

After tempering at a 200°C for 120 min, the structure of steel becomes more homogeneous (Fig. 3c). Rockwell hardness is slightly reduced to ~49HRC. This may be due to the partial decomposition of martensite and the formation of microdispersed carbide phase  $Fe_xC$  [4]. When the tempering temperature increases to 400°C, the grain boundaries became fuzzy gradually. It can be explained by further precipitation of carbon from the supersaturated  $\alpha$ -solid solution and coagulation of carbide particles. Structure of

tempered at 400°C steel is troostite. The carbide precipitations could be seen clearly (as shown in the image at the bottom right corner in Fig. 3d). The hardness decreases to ~32HRC. After the tempering at a temperature of 600°C, the steel structure consists of a composition of granular 314orbate and ferrite. The hardness is ~28 HRC.

### 3.2. Micromechanical properties

The results of 30MnB5 steel dynamic indentation are presented in Table 3.

**Table 3.** Micromechanical properties of steel 30MnB5 different structure.

	H [GPa]	$h_{max}$ , [ $\mu m$ ]	$A_{plast}$ [ $10^{-8}$ J]	$A_{elast}$ [ $10^{-8}$ J]
a*	4.238	2.1	41.25	8.94
b	10.833	1.2	29.25	8.06
c	10.160	1.26	29.42	7.94
d	5.795	1.7	36.67	9.21
e	4.578	1.9	43.35	8.72

\*a - delivery state; b - quenching in water from a temperature of 900°C; c - quenching and tempering at 200°C, d - quenching and tempering at 400°C, e - quenching and tempering at 600°C.

Maximal penetration of the Berkovich pyramid into the 30MnB5 steel in the delivery state is  $h_{max} \sim 2.1 \mu m$  (Fig. 4).

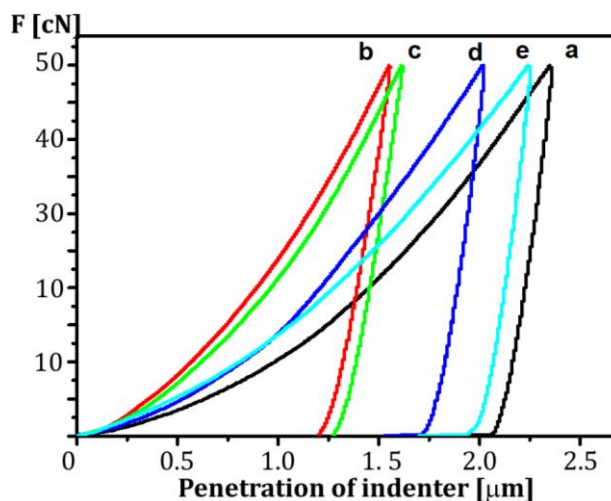


**Fig. 4.** Curves of dynamic indentation of steel 30MnB5 (average curve from 5 tests). a - delivery state; b - quenching in water from a temperature of 900°C; c - quenching and tempering at 200°C, d - quenching and tempering at 400°C, e - quenching and tempering at 600°C.

The ferritic-pearlite structure has the lowest micro hardness (~4,238 GPa) and maximal work of plastic deformation (~41.25·10<sup>-8</sup>).

After quenching, the penetration of the indenter into the martensitic structure significantly reduces (Fig. 4b), the work of plastic deformation decreases by 30% (Table 3). The microhardness increases by more than 2 times (Table 3).

The indentation deep increases after the tempering of steel. The penetration of indenter into tempered at 200°C steel increases only by ~5%. Accordingly, work of steel deformation changes insignificantly: work of plastic deformation increases by ~5% and elastic – decreases by ~2%. After tempering of steel at 200°C its microhardness decreases by ~7% (Table 3).

After tempering of steel at 400°C penetration of indenter increases by 40% compared to quenched steel, microhardness decreases almost twice, work of plastic deformation exceeds work of elastic deformation. It illustrates the increase in plasticity of the material. This trend is observed after annealing at 600°C. Compared to quenched steel, deep of indenter increases by ~60% and microhardness decreases by ~58% (Fig. 4, Table 3).

The work of elastic deformation has no clear dependence on the tempering temperature and changes insignificantly (up to 15%). The work of plastic deformation enhances, when tempering temperature increases.

### 3.3. Tribological properties

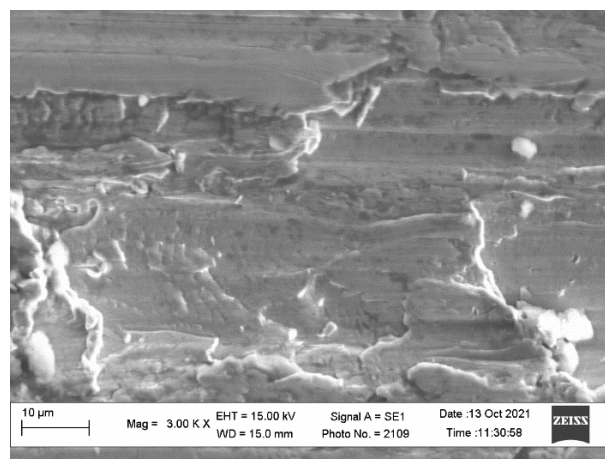
#### Friction tests with a fixed abrasive.

The wear of steel 30MnB5 in delivery state after friction tests with a fixed abrasive is a result of microcutting and pulling out of the surface. Numerous signs of adhesive interaction of the contact surfaces were found (Fig. 5a).

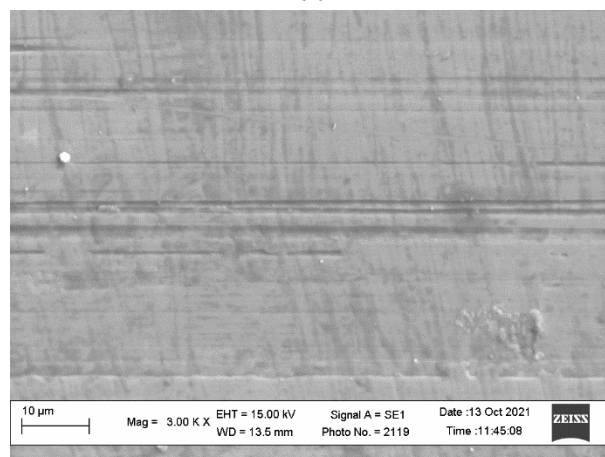
After quenching of steel the damage of the friction surface is significantly reduced. Surface is smooth, local scratches <1 μm wide with smooth edges are detected. No signs of plastic deformation were found (Fig. 5b).

After tempering at a temperature of 200°C, the damage at the friction surface is similar to one after quenching. Local scratches occurs as a result of micro-ploughing of the surface by abrasive particles due to their sliding and rolling (Fig. 5c).

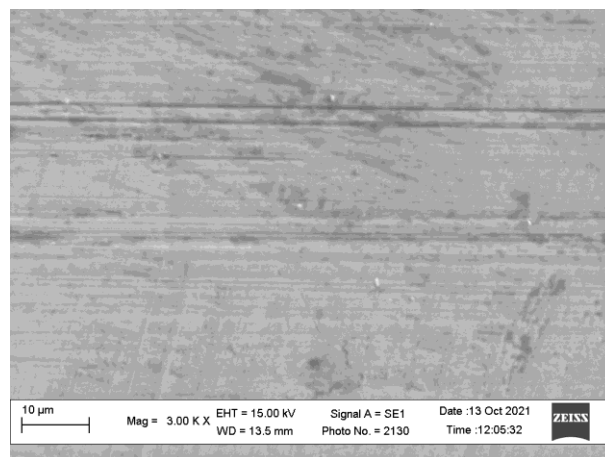
After tempering at a temperature of 400°C, the topography of the friction surface changes sharply and it indicates the decrease of wear resistance of the material. The width of the scratches increases significantly, which indicates an increase in the depth of damage. The adhesive pits and uneven edges of the friction track are observed, which illustrates the increase in plasticity of the material and local adhesion between the contact surfaces (Fig. 5d).



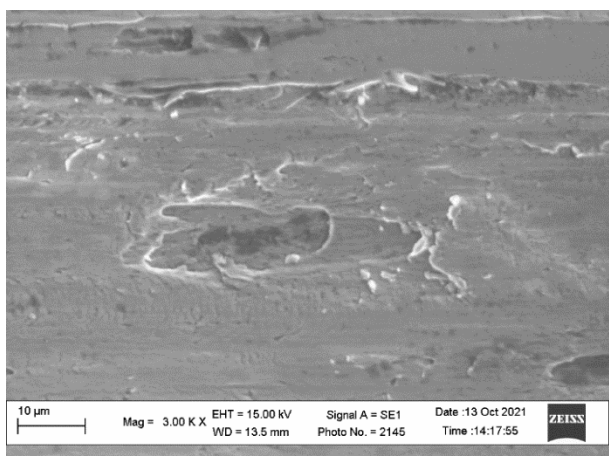
(a)



(b)



(c)



(d)

**Fig. 5.** Surface of steel 30MnB5 after friction tests with a fixed abrasive: (a) - in delivery state; (b) - quenching in water from a temperature of 900°C; (c) - quenching and tempering at 200°C; (d) - quenching and tempering at 400°C; ×3000.

Abrasive particles stuck and embedded in the plastically deformed friction surface, were found. Silica particles can increase the wear of steel. Significant weight loss (~0.079 g/cm<sup>2</sup>) of the tempered at 600°C steel was detected after 15 min friction test (Fig. 6a).

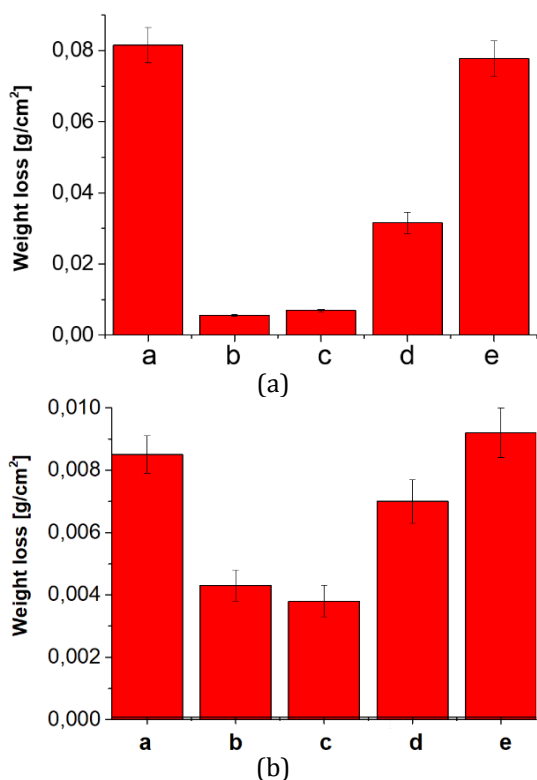


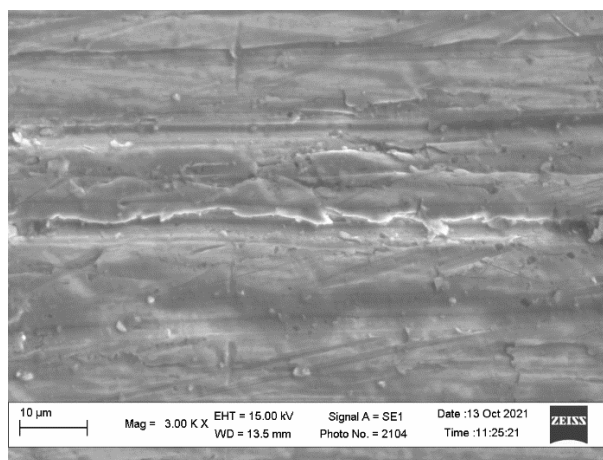
**Fig. 6.** Weight losses of 30MnB5 steel at the friction tests with fixed abrasive (a) and unfixed abrasive (b): a - delivery state; b - quenching in water from a temperature of 900°C; c - quenching and tempering at 200°C, d - quenching and tempering at 400°C, e - quenching and tempering at 600°C.

### Friction tests with a unfixed abrasive.

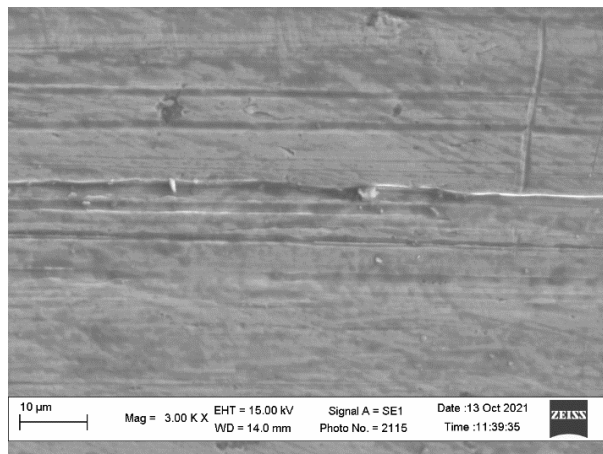
The numerous scratches with uneven edges are observed at the friction surface of the steel 30MnB5 in the delivery state after friction test with unfixed particles of abrasive (Fig. 7a). The worn surface was plastic deformed during the wear process. Numerous abrasive particles stuck and embedded in the plastically deformed friction surface was observed. The presence of a layer with fixed particles can increase wear or protect the bulk material and decrease the wear rate [2].

The width and depth of the friction track reduces after quenching of the steel and surface strengthening. The micro-cutting of the surface by abrasive particles and single chipping of grains were observed. The boundaries of the track are clear, without signs of plastic deformation (Fig. 7b).

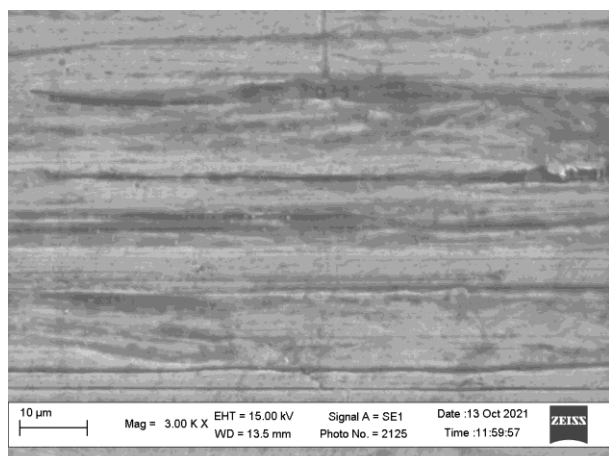
After tempering at a temperature of 200°C, the damage of the friction surface is similar. There are traces of micro cutting, sliding, and rolling of abrasive particles on the surface (Fig. 7c).



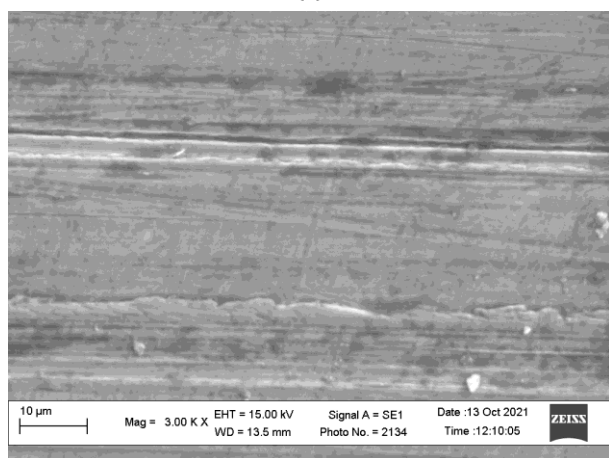
(a)



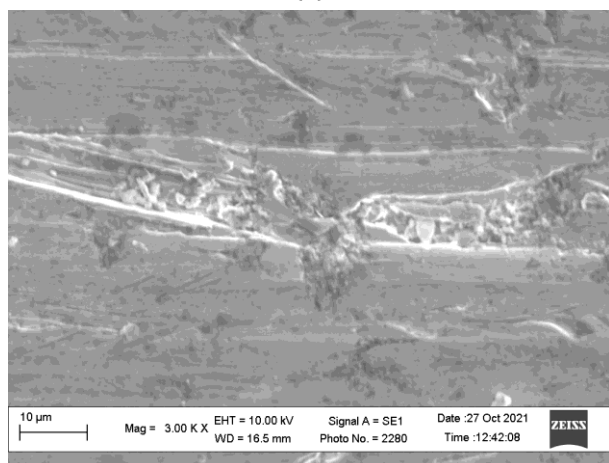
(b)



(c)



(d)



(e)

**Fig. 7.** Surface of steel 30MnB5 after friction tests with unfixed abrasive: (a) - in delivery state; (b) - quenching in water from a temperature of 900°C; (c) - quenching and tempering at 200°C; (d) - quenching and tempering at 400°C; (e) - quenching and tempering at 600°C;  $\times 3000$ .

After tempering at 400°C, the width of the wear track increases by 3-10 times. Wear occurs mainly in a result of micro-cutting.

The brittle destruction of the surface and traces of adhesion between the contacting surfaces were not detected (Fig. 7d).

The damage of the friction surface significantly increases after tempering of steel at 600°C. Wear is a result of micro-plowing simultaneously with the plastic deformation and displacement of material from the grooves. Particles of abrasive are observed in the grooves too.

The weight loss of steel at the friction test with an unfixed abrasive (Fig. 6b) is an order of magnitude less than in the case of a fixed abrasive due to the less stringent friction conditions. The best wear resistance is obtained after quenching of steel and after quenching and after tempering at 200°C of quenched steel (Fig. 6b). The weight losses increase after tempering at 400 and 600°C by  $\sim 1.8$  and  $\sim 2.4$  times respectively. Under these conditions, the increase in tempering temperature does not have such an effect on the wear resistance of steel, as in the case of friction with a fixed abrasive.

#### Sclerometric studies.

The results of sclerometric studies are presented in Fig. 8, 9 and Table 3. The average value of the friction coefficient at the movement of the indenter on 30MnB5 steel in the delivery state is  $0.14 \pm 0.008$ . Oscillation of friction coefficient relates to different micromechanical properties of structural components: adhesion of indenter decreases at the contact with ferrite and increases at the contact with pearlite. Track with depth  $\sim 4 \mu\text{m}$  and width  $\sim 40 \mu\text{m}$  is formed. There is a significant plastic displacement of material along the edges of the track, which is also associated with different characteristics of elasticity and ductility of ferrite and pearlite.

The coefficient of friction decreases to  $\sim 0.132 \pm 0.003$  after quenching of steel. A little oscillation of friction coefficient is observed. This is due to a 2.5-fold increase in microhardness and a significantly smaller penetration of the indenter into the material (track depth  $\sim 1.3 \mu\text{m}$ ) (Fig. 9). Uneven removal of material from friction zone due to shredding is observed.

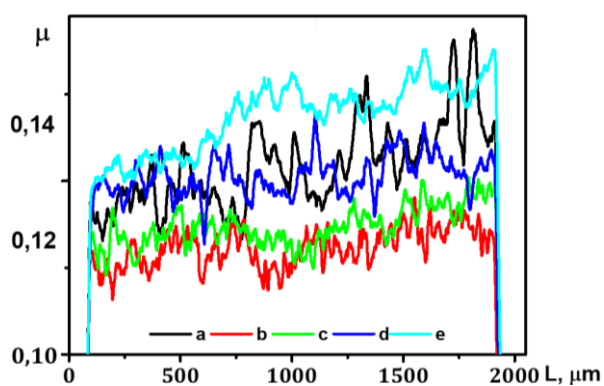
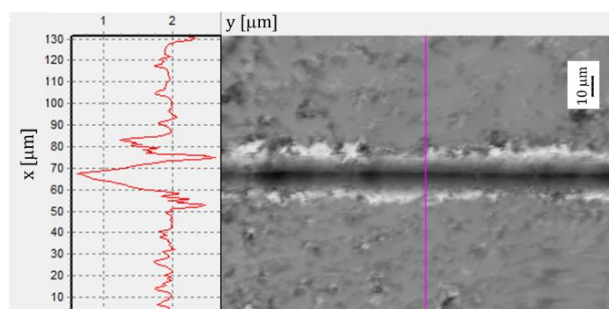
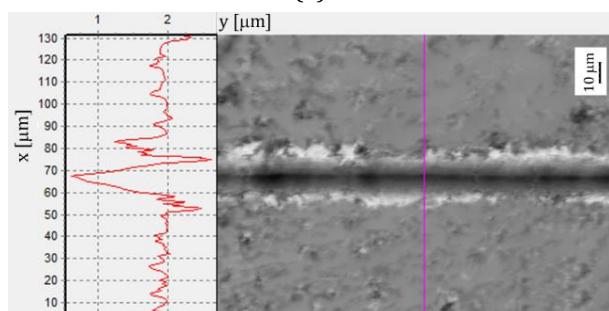


**Fig. 8.** Coefficient of friction of 30MnB5 steel at the scratch test: (a) - delivery state; (b) - quenching at 900°C; (c) - quenching and tempering at 200°C, (d) - quenching and tempering at 400°C, (e) - quenching and tempering at 600°C.

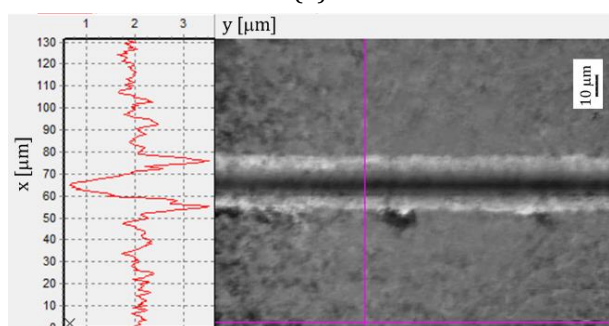
After tempering of steel at 200°C the track depth and width do not change, but removal of material along the edges of the track is smoother and more uniform. After tempering at 400 and 600°C, the coefficient of friction increases to ~0.14 and ~0.15, respectively (Fig. 8).



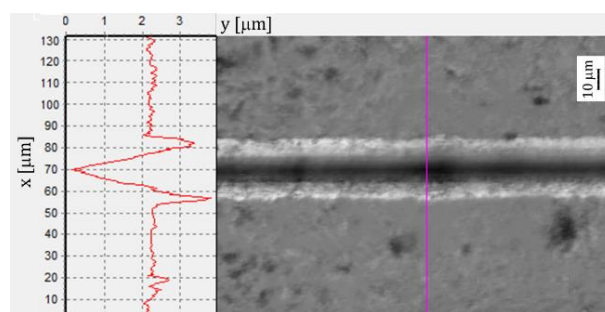
(a)



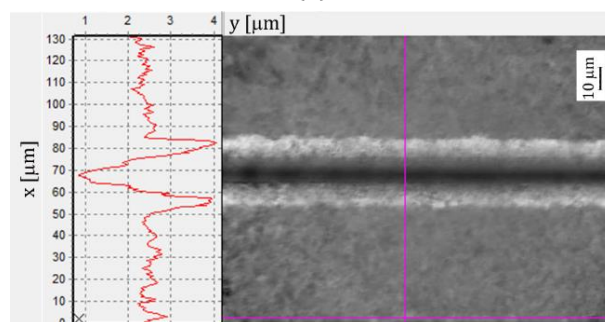
(b)



(c)



(d)



(e)

**Fig. 9.** Images and profiles of 30MnB5 steel tracks after scratch test: (a) - delivery state; (b) - quenching in water from a temperature of 900°C; (c) - quenching and tempering at 200°C, (d) - quenching and tempering at 400°C, (e) - quenching and tempering at 600°C.

The depth and width of the track increase almost twice. The release of material from the contact zone for steel after tempering at both temperatures is uniform along the track.

Parameters of scratch profile indicate that volume of released material increases, when tempering temperature increases from 400°C to 600°C (Fig. 9d, e).

## 4. DISCUSSION

### Microstructure

Tempering after quenching is a significant process for steels to obtain optimal mechanical properties [4]. The microstructure morphologies of the steels tempered at different temperatures are presented in Figure 3. After quenching from a temperature of 900°C the microstructure of the steel mainly consists of martensite. After the tempering the decomposition of martensite, the separation and growth of carbides is observed. When the steel is tempered at low temperature (200°C), the diffusion velocity of carbon is slow. The result of tempering is the partial decomposition of martensite and a decrease in internal stresses. Rockwell hardness and microhardness are slightly reduced.

When the tempering temperature increases, the diffusion velocity of carbon accelerates. It can accelerate the decomposition of martensite and separation of carbides [4]. The decreasing tendency of hardness is observed, as a tempering temperature increase. After tempering at 600°C hardness and microhardness reduces almost twice.

### **Relationship between mechanical properties and wear resistance**

The friction test of 30MnB5 steel with fixed abrasive shows that the weight loss correlates with the hardness of the material (Table 2). The hardness of steel strongly increases after quenching and the weight loss is ~15 times smaller compared to initial state. After tempering at 200°C, the hardness of the steel decreases and its wear increases insignificantly. After the tempering at the temperature 400 and 600°C, the hardness of steel decreases almost twice and the mass losses increase more than 4 times.

Wear resistance of steel at friction test with the fixed abrasive depends on its microhardness which provides resistance of material to microcutting by abrasive grain.

The total weight loss is an order of magnitude less than in the case of a fixed abrasive due to the change in the friction conditions. The smallest mass losses are observed after quenching and quenching with tempering at 200°C. The increase in tempering temperature does not have such an effect on the wear resistance of steel, as in the case of friction with a fixed abrasive.

Unfixed abrasive particles are involved in load perception and could wedge into the friction surface, grind into softer fractions, roll along the wear surface, and resiliently and plastically deform it [2]. Therefore, wear resistance of steel is less dependent on hardness, than on the magnitude and distribution of internal stresses in the crystal lattice of the metal.

### **Relationship between the results of sclerometry and the wear resistance**

Scratch test can be considered as a single act of friction, allows to evaluate the nature of damage and pressing-out of the material of contact zone between indenter and metal surface. It also can be applied for determination of the friction force and surface fracture resistance under interaction.

The width and depth of the scratch depends on plastic-elastic properties of steel. When the tempering temperature of steel increases, work of plastic deformation grows, but the work of elastic deformation is almost stable. It was found that wear resistance of steel reduces, when the work of plastic deformation increases. Uneven removal of material from friction zone due to shredding is observed in quenched steel. After tempering of steel, the removal of material along the edges of the track is smoother and uniform. Volume of removed material correlates with the work of plastic deformation.

This makes it possible to use sclerometry as an express method for testing steel for wear resistance after various types of heat treatment.

### **Wear mechanisms at the friction tests with a fixed abrasive**

The formation of the narrow and shallow grooves is observed on the friction surface of steel 30MnB5 after quenching and tempering at 200°C. Grooves are oriented parallel to the direction of sliding. The main mechanisms of wear are micro-cutting and micro-ploughing. The micro-chip removal is observed on the surface of quenched steel. After tempering the micro-cutting decreases.

The abrasive wear of tempered at 400°C and 600°C steel is the result of micro-cutting and micro-ploughing simultaneously with plastic deformation and displacement of material along the grooves. Some pit holes with the pronounced "lips" at the rear end are found on the surface in a result of abraders penetration. Surface damage increases after the tempering of steel at 600°C.

### **Wear mechanisms at the friction tests with an unfixed abrasive**

Surface damage is less than under friction with a fixed abrasive. Micro-cutting and micro-ploughing are the main wear mechanisms of quenched and tempered at 200°C steel 30MnB5. The displacement of material along the grooves and its plastic deformation are observed on the friction surface of steel after tempering at 400°C. Wear of tempered at 600 °C additionally is a result of micro-ploughing simultaneously with the plastic deformation and displacement of material from the grooves. Embedded particles of abrasive are observed in the plastically deformed surface of grooves.

## 5. CONCLUSIONS

The microstructure evolution of the 30MnB5 steel, tempered at different temperatures, the micromechanical properties and wear resistance was studied.

1. With tempering temperature increasing from 200°C to 400°C and 600°C, the carbon precipitations separated out constantly, coagulation and increase of grain size are observed. The microstructure of tempered at 200°C steel consists of tempered martensite and ferrite. After tempering at 400°C martensite transformed to troostite and at 600°C – to sorbite.
2. The abrasive wear resistance of 30MnB5 steel depends on its hardness which provides resistance of material to micro-cutting by abrasive grain. Maximal wear resistance of steel is observed after quenching and tempering at 200°C, when its hardness is 54 and 49 HRC.
3. The correlation between results of sclerometry and nano-indentation and wear resistance of steel was found. Minimal work of plastic deformation at the nano-indentation ( $29.42 \cdot 10^{-8}$  J) correlates with the maximal wear resistance of steel. This makes it possible to use sclerometry as an express method for testing steel for wear resistance after various types of heat treatment.
4. The abrasive wear of quenched and tempered at 200°C steel 30MnB5 is the result of micro-cutting and micro-ploughing. The plastic deformation, displacement of material along the grooves, pit holes are observed on the friction surface of steel after tempering at 400°C and 600°C. Surface damage at the friction tests with an unfixed abrasive is less than with a fixed abrasive.

## REFERENCES

[1] K. Pawlak, B. Białobrzaska, Ł. Konat, *The influence of austenitizing temperature on prior austenite grain size and resistance to abrasion wear of selected low-alloy boron steel*, Archives of civil and mechanical engineering, vol. 16, iss. 4, pp. 913-926, 2016, doi: [10.1016/j.acme.2016.07.003](https://doi.org/10.1016/j.acme.2016.07.003)

[2] S. Hernandez, J. Hardell, H. Winkelmann, M.R. Ripoll, B. Prakash, *Influence of temperature on abrasive wear of boron steel and hot forming tool steel*, Wear, vol. 338-339, pp. 27-35, 2015, doi: [10.1016/j.wear.2015.05.010](https://doi.org/10.1016/j.wear.2015.05.010)

[3] O. Haiko, K. Valtonen, A. Kaijalainen, S. Uusikallio, J. Hannula, T. Liimatainen, J. Kömi, *Effect of tempering on the impact-abrasive and abrasive wear resistance of ultra-high strength steels*, Wear, vol. 440-441, pp. 1-11, 2019, doi: [10.1016/j.wear.2019.203098](https://doi.org/10.1016/j.wear.2019.203098)

[4] E. Wen, R. Song, W. Xiong, *Effect of tempering temperature on microstructures and wear behavior of a 500 HB grade wear-resistant steel*, Metals, vol. 9, iss. 1, pp. 1-14, 2019, doi: [10.3390/met9010045](https://doi.org/10.3390/met9010045)

[5] P. Cardei, L. Vladutoiu, G. Chisuiu, A. Tudor, C. Sorica, M. Gheres, S. Muraru, *Research on friction influence on the working process of agricultural machines for soil tillage*, Materials Science and Engineering, vol. 444, pp. 1-10, 2018, doi: [10.1088/1757-899x/444/2/022014](https://doi.org/10.1088/1757-899x/444/2/022014)

[6] X. Qiang, F. Bijlaard, H. Kolstein, *Dependence of mechanical properties of high strength steel S690 on elevated temperatures*, Construction and Building Materials, vol. 30, pp. 73-79, 2012, doi: [10.1016/j.conbuildmat.2011.12.018](https://doi.org/10.1016/j.conbuildmat.2011.12.018)

[7] C. Löbbe, O. Hering, L. Hiegemann, A. Tekkaya, *Setting Mechanical Properties of High Strength Steels for Rapid Hot Forming Processes*, Materials, vol. 9, iss. 4, pp. 1-19, 2016, doi: [10.3390/ma9040229](https://doi.org/10.3390/ma9040229)

[8] F.P.A. Robinson, W.G. Scurr, *Effect of boron on the corrosion resistance of austenitic stainless steels*, Corrosion, vol. 33, iss. 11, pp. 408-417, 1977, doi: [10.5006/0010-9312-33.11.408](https://doi.org/10.5006/0010-9312-33.11.408)

[9] S.P. Ruan, A.M. Zhao, Y.C. Li, M.Y. Guo, Z.Y. Song, *Effect of Boron and Chromium on Hardenability in 0.33% C Cold Heading Steel*, Materials Science Forum, vol. 867, pp. 24-28, 2016, doi: [10.4028/www.scientific.net/msf.867.24](https://doi.org/10.4028/www.scientific.net/msf.867.24)

[10] T.I. Titova, N.A. Shulgan, I.Yu. Malykhina, *Effect of boron microalloying on the structure and hardenability of building steel*, Metal Science and Heat Treatment, vol. 49, iss 1-2, pp. 39-44, 2007, doi: [10.1007/s11041-007-0007-8](https://doi.org/10.1007/s11041-007-0007-8)

[11] V.V. Parusov, A.B. Sychkov, I.V. Derevianchenko, M.A. Jygarev, *New application of boron in metallurgy*, Bulletin of Magnitogorsk State Technical University, vol. 9, no. 1, 2005. (in Russian)

[12] N. Ojala, K. Valtonen, V. Heino, M. Kallio, J. Aaltonen, P. Siitonen, V. Kuokkala, *Effects of composition and microstructure on the abrasive wear performance of quenched wear resistant steels*, Wear, vol. 317, iss. 1-2, pp. 225-232, 2014, doi: [10.1016/j.wear.2014.06.003](https://doi.org/10.1016/j.wear.2014.06.003)

- [13] H. Güler, R. Ertan, R. Ozcan, *Characteristics of 30MnB5 boron steel at elevated temperatures*, Materials Science and Engineering, vol. 578, pp. 417–421, doi: [10.1016/j.msea.2013.04.116](https://doi.org/10.1016/j.msea.2013.04.116)
- [14] Yu.I. Golovin, *Nanoindentation and mechanical properties of solids in submicrovolumes, thin near-surface layers, and films: A Review*, Physics of the Solid State, vol. 50, iss. 12, pp. 2205–2236, 2008, doi: [10.1134/S1063783408120019](https://doi.org/10.1134/S1063783408120019)
- [15] P.J. Blau, *Lab Handbook of Scratch Testing, Chapter 7, Scratch Adhesion Testing*, Blue Rock Technical Publication, Oak Ridge, TN, pp. 7.1-7.15, 2002.
- [16] S.R. Ignatovich, I.M. Zakiev, *Universal micronanoindentermeter Micron-gamma*, Industrial Laboratory, Materials Diagnostics, vol. 77, pp. 61–67, 2011. (in Russian)
- [17] G.W. Queirós, J. Bermejo, L.G. Sanchez, J.M. Gómez de Salazar, A.J. Criado, *Improvement of the Mechanical Properties of 30MnB5 Wear-Resistant Steel by Subcritical Annealing and Water Quenching, Improving Its Life Cycle Analysis*, Journal of Material Science & Engineering, vol. 7, iss. 5, pp. 1-3, 2018, doi: [10.4172/2169-0022.1000495](https://doi.org/10.4172/2169-0022.1000495)
- [18] A. Yazici, *Investigation of the Wear Behavior of Martempered 30MnB5 Steel for Soil Tillage*, Transactions of the ASABE, vol. 55, pp.15-20, 2012, doi: [10.13031/2013.41243](https://doi.org/10.13031/2013.41243)
- [19] E. Baradyntseva, N.A. Glazunova, O.V. Rogovtsova, *Influence of microalloying by boron on hardenability of steel*, Casting and metallurgy, vol. 84, no. 3, pp. 70-74, 2016. (in Russian)
- [20] M.G. Gee, A. Gant, I.M. Hutchings, *Rotating Wheel Abrasive Wear Testing*, Teddington: University of Cambridge, available at <https://eprintspublications.npl.co.uk/2543/1/mgpg55.pdf>